STING Agonist Enhances the Efficacy of PD-L1 Monoclonal Antibody in Breast Cancer Immunotherapy by Activating the IFNβ Signaling Pathway

Mingming Yin
Anhiu No.2 Provincial People's Hospital
Jinlong Hu
Anhiu No.2 Provincial People's Hospital
Zhongxu Yuan
Anhiu No.2 Provincial People's Hospital
Guangyi Luo
Anhiu No.2 Provincial People's Hospital
Jiaming Yao
Anhiu No.2 Provincial People's Hospital,
Rundong Wang
Anhiu No.2 Provincial People's Hospital,
Dongquan Liu
Anhiu No.2 Provincial People's Hospital
Baoqiang Cao
Anhiu No.2 Provincial People's Hospital
Zhiqi Hu
Anhiu No.2 Provincial People's Hospital
Wenyong Wu (wenyong_wu1977@163.com)
Anhiu No.2 Provincial People's Hospital https://orcid.org/0000-0003-0282-9042

Research Article

Keywords: BCa immunotherapy, STING agonist, Atezolizumab, PD-L1, IFNβ

Posted Date: September 21st, 2021

DOI: https://doi.org/10.21203/rs.3.rs-914487/v1

Abstract

Purpose: This article focused on STING agonist role in breast cancer (BCa) immunotherapy.

Methods: Clinical samples were collected from 37 BCa patients'. Xenograft tumor model was established by injecting 4T1 cells into mammary fat pad of mice. STING agonist and Atezolizumab were injected into mice with 2 times a week for 2 weeks. Peripheral blood, xenograft tumor, lung, liver, brain-cortex and kidney of mice were collected. Anti-IFNAR1 was used to treat 4T1 cells. Quantitative reverse transcription-polymerase chain reaction and Western blot were used for mRNA and proteins expression. Enzyme-linked immunosorbent assay, immunohistochemistry and hematoxylin-eosin staining were performed.

Results: Tumor tissues of BCa patients exhibited lower STING and high PD-1 and PD-L1 protein expression. STING agonist inhibited 4T1 cells growth in mice ($P < 0.001$). STING agonist increased IFNβ level and the phosphorylation of STING, TBK1, IRF3 and STAT1 in xenograft tumor ($P < 0.001$). STING agonist synergized with Atezolizumab to inhibit 4T1 cells growth in mice, and increase TNF-α, IFN-β and IL-10 level in peripheral blood and xenograft tumor ($P < 0.01$). STING agonist synergized with Atezolizumab to increase CD8+ cytotoxic T cells and decrease FOXP3+ Tregs cells in xenograft tumor. STING agonist was non-toxic to lung, liver, brain-cortex and kidney. Anti-IFNAR1 reversed STING agonist promotion on TBK1, IRF3 and STAT1 phosphorylation in 4T1 cells ($P < 0.01$).

Conclusion: STING agonist enhances the efficacy of Atezolizumab in BCa immunotherapy by activating the IFNβ signaling pathway.

Highlights

(1) BCa patients had low STING and high PD-1 and PD-L1 proteins expression.

(2) STING agonist inhibited 4T1 cells growth and promoted IFNβ expression in mice.

(3) STING agonist synergized with Atezolizumab to inhibit 4T1 cells growth in mice.

(4) STING agonist had anti-tumor effect in BCa through activating IFNβ pathway.

Introduction

Breast cancer (BCa) is a main malignant tumor that often occurs in women. BCa is the major reason of cancer related death in women all over the world [1]. About 30% of all new diagnosed cancer patients were identifies as BCa, and 15% of all cancer-related deaths were due to BCa in women [2]. Surgical resection, chemotherapy and radiotherapy are traditional treatments for BCa. However, the mortality rate remains at a high level due to metastasis and relapse caused by treatment resistance [3].

Immunotherapy is a newly emerged treatment strategy of solid tumor, which emergence is gradually changing the traditional treatment concept of solid tumors [4]. Programmed death-1 (PD-1) and

programmed death-ligand 1 (PD-L1) are identified as immunotherapy targets for cancers [5, 6]. PD-1 is expressed by activated T cells while PD-L1 is expressed by tumor cells [6]. PD-1, acted as a cell surface receptor, can suppress the activation of T cell though binding to PD-L1, thereby promoting immune escape of tumor cells [7]. Researches have indicated that the blockage between PD-1 and PD-L1 can enhance the response of T cells to facilitate antitumor activity [8, 9]. Available data has been indicated that the PD-1/PD-L1 antagonists possess clinical activity in some BCa patients [4]. In 2019, Atezolizumab (a kind of PD-L1 monoclonal antibody) became the first immune checkpoint inhibitor approved specifically for BCa [10, 11]. It greatly improved BCa patients' progression-free survival and overall survival, but also was approved for the treatment of PD-L1-positive triple-negative breast cancer patients [10, 12, 13].

Stimulator of interferon genes (STING), which is considered as a cytosolic pattern recognition receptor, is very important for the spontaneous induction of anti-tumor T cell immunity [14]. It has been found that STING activation can activate anti-tumor T cells through stimulating type I interferon (IFN-I)-mediated inflammation program [15]. Thus, it is inferred that the activation of STING may be an effective way to enhance the immunotherapy effect of tumors. Studies have found that STING agonist can enhance the immunotherapy effect of BCa [16]. Meanwhile, STING agonist treatment can normalize BCa microenvironment, which obvious enhances the regression of immunotherapy-resistant BCa in the present of immune checkpoint blockade [17]. However, whether STING agonist can enhance the efficacy of Atezolizumab in BCa is still rarely reported. Thus, this study researched the function of STING agonist in BCa treatment by Atezolizumab. Importantly, the mechanism involved in this process was also explored. It was hoped that this study could provide solid theoretical basis for BCa treatment by Atezolizumab in the clinic.

Methods

Clinical samples collection

In this study, a total of 37 BCa patients' tumor tissues and paired adjacent normal tissues were collected. All of these patients were firstly diagnosed with BCa, without previous history of cancer-related diseases or treatment. The clinical tissues were stored at -80°C in a refrigerator.

This research has been approved by the ethics committee of Anhiu No.2 Provincial People’s Hospital and complied with the Declaration of Helsinki. All patients have signed written informed consent and voluntarily joined the study.

Cells and culture

Mice BCa cell line (4T1) was commercially provided by the American Type Culture Collection (ATCC, Manassas, Virginia, USA). The cell line was cultured at 37°C, 5% CO_2 in dulbecco's modified eagle medium (DMEM) containing 10% fetal bovine serum (FBS).

Animals and xenograft tumor model

Animal study has been approved by the animal ethics committee of Anhiu No.2 Provincial People's Hospital. Female Balb/c mice (n = 20, 5 weeks old) were purchased from Shanghai Laboratory Animal Center of Chinese Academy of Sciences (Shanghai, China). Mice were housed in a (22 ± 1)°C and 12-h day/night cycle room. Food and water was freely available. Mice were randomly divided into 4 groups: Vehicle group, STING agonist group, Atezolizumab group and STING agonist + Atezolizumab group. For each group, 5 mice were included. The treatment of mice in each group was as follows:

Firstly, 4T1 cells were collected when the confluence researched to about 85%. Phosphate-buffer saline (PBS) was used to disperse 4T1 cells to a density of 1×10^7 cells/mL. Then 4T1 cells suspension (100 μL) was injected into the mammary fat pad of mice in each group. Five days after 4T1 cells injection, STING agonist (25 μg) was injected into the tumor mass of mice in STING agonist group. At the same time point, mice of PBS group were injected with a vehicle of PBS. Mice of Atezolizumab group were injected intraperitoneally with Atezolizumab (200 μg). Meanwhile, mice of STING agonist + Atezolizumab group were not only injected with STING agonist (25 μg) into the tumor mass, but also injected intraperitoneally with Atezolizumab (200 μg). The injection frequency of STING agonist and Atezolizumab was 2 times a week and injected for 2 weeks.

Furthermore, on the 1st, 7th and 14th day after injection of PBS, STING agonist, Atezolizumab or both STING agonist and Atezolizumab, peripheral blood of mice in each group was collected from orbit and stored at -80°C in a refrigerator. The peripheral blood collection time was 4 h after injection.

From the 5th day of 4T1 cells injection, the tumor volume was measured every 3 days with the following formula: $V = 0.5 \times \text{length} \times \text{width}^2$. On the 29th day after 4T1 cells injection, mice were anesthetized by 2% isoflurane and then killed through cervical dislocation. The xenograft tumor mass was collected from mice and stored at -80°C in a refrigerator [18, 19]. Additionally, lung, liver, brain-cortex and kidney of mice were also collected and stored at -80°C in a refrigerator.

Anti-IFNART treatment of 4T1 cells

When reached to about 85% confluence, 4T1 cells were harvested and dispersed into DMEM containing 10% FBS (1×10^6 cells/mL). A total of 1 mL cells suspension was contained per well. After that, STING agonist was added into 4T1 cells to a final concentration of 100 μg/mL (named STING agonist group). STING agonist (final concentration 100 μg/mL) and anti-IFNART (final concentration 10 ng/mL) were both used to treat 4T1 cells (named STING agonist + anti-IFNART group). 4T1 cells treated by PBS (final concentration 100 μg/mL) were used as Vehicle group. Cells were cultured for 48 h at 37°C, 5% CO_2, followed by being collected to subjected to Western blot.

Enzyme-linked immunosorbent assay (ELISA)

The xenograft tumor mass was homogenized at 15000 r/min for 40 s, followed by being centrifuged at 1000 r/min for 5 min. The supernatant was collected. Using an ELISA kit, the level of TNF-α, IFN-β and IL-10 in peripheral blood samples and the above supernatant was detected in line with the instructions.

Quantitative reverse transcription-polymerase chain reaction (qRT-PCR)

Clinical samples and xenograft tumor mass was prepared into powder in liquid nitrogen. Total RNA in tissue powder samples was extracted using TRIzol reagent (Beyotime, Shanghai, China). The extraction procedures were strictly based on the instructions. Thereafter, cDNA was synthesized using 2 μg of total RNA samples according to the instruction of the Roche Transcriptor First Strand cDNA Synthesis kit (Roche, Mannheim, Germany). The cDNA was subjected to PCR using the ABI7500 instrument (Applied Biosystems, Waltham, MA, USA) in line with the following procedure: 95˚C for 5 min, 38 cycles of (95˚C for 45 s, 50˚C for 45 s and 72˚C for 40 s), and 72˚C for 3 min. Genes and corresponding primers were: STING, forward 5'-CAAGGACCAACTACAACC-3', reverse 5'-TGCCTCTTCTTTAATTG-3'. PD-1, forward 5'-GGTGTGAGGCCATCCACAA-3', reverse 5'-CCATTCTGTCGGAGCCTCTG-3'. PD-L1, forward 5'-TATGGTGGTGCCGACTACAA-3', reverse 5'-TGGCTCCCAGAATTACCAAG-3'. TNF-α, forward 5'-CCCGCATCCCAGGACCTCTCT-3', reverse 5'-CGGGGGACTGGCGA-3'. IFN-β, forward 5'-TCCGAGCAGAGATCTTCAGGAA-3', reverse 5'-TGCAACCA-CCACTCATTCTGAG-3'. IL-10, forward 5'-CTTCGAGATCTCCGAGATGCCTTC-3', reverse 5'-ATTCTTCACCTGCTCCACGGCCTT-3'. Actin, forward 5'-TCCTGTGGCATCCACGAAAC-3', reverse 5'-GAAGCATTTGCGGACGAT-3'. Actin was used as control to normalize the expression of other mRNA expression by $2^{-\Delta\Delta CT}$ method.

Immunohistochemistry (IHC)

Clinical samples and xenograft tumor mass were treated by 10% formaldehyde solution for 24 h. Paraffin was used to embed tissues and then tissues were cut into sections (4 μm). Sections were sequentially treated by xylene and gradient alcohol for dewaxing and rehydration. Antigen retrieval was carried out by immersing sections into citrate buffer (10 mM, pH = 6.0). After 10 min treating with 3% H_2O_2, sections were treated for 1 h with 5% goat serum. Primary antibodies (1:100) were added to treat section for 12 at 4˚C. Primary antibodies were: rabbit anti-STING (ab252560, Abcam, Shanghai, China), rabbit anti-PD-L1 (ab233482, Abcam, Shanghai, China), mouse anti-PD-1 (ab52587, Abcam, Shanghai, China), rabbit anti-CD8+ (ab138727, Abcam, Shanghai, China) and rabbit anti-FOXP3+ (ab4728, Abcam, Shanghai, China). Goat anti-rabbit (ab150080, Abcam, Shanghai, China) or anti-mouse (ab6789, Abcam, Shanghai, China) secondary antibodies (1:200) was then applied for 2 h treating of sections. Diaminobenzidine (DAB) (Solarbio, Beijing, China)was used to stain sections, followed by hematoxylin staining (Solarbio, Beijing, China). Dehydration of sections was performed using gradient alcohol. Transparency of sections was carried out by xylene. After sealed in neutral resin, sections were observed using a microscope.

Hematoxylin-eosin (HE) staining

As described above, mice lung, liver, brain-cortex and kidney were treated by 10% formaldehyde solution for 24 h. Tissues embedded into paraffin were prepared into sections (4 μm), followed by treated with xylene and gradient alcohol for dewaxing and rehydration. According to instructions, hematoxylin and eosin (Solarbio, Beijing, China) were sequentially applied for sections staining. Dehydration and

transparency was conducted by using gradient alcohol and xylene. After sealed in neutral resin, sections were observed using a microscope.

Western blot

Xenograft tumor mass was prepared into powder in liquid nitrogen to extract total proteins using lysis buffer (Beyotime, Shanghai, China) on ice. Additionally, 4T1 cells were lysed by lysis buffer. Total proteins in the supernatant were collected after centrifuged at 5000 × g, 20 min. The concentration of total proteins was determined using a BCA kit (Beyotime, Shanghai, China) according to the instructions. After that, 20 μg of protein sample was experienced separation using 10% sodium dodecyl sulfate-polyacrylamide gel electrophoresis (SDS-PAGE). After being separated, proteins were transferred onto a polyvinylidene fluoride (PVDF) membrane. For blocking, 5% skimmed milk was used to incubate the PVDF membrane for 1 h. TBS containing 0.1% Tween-20 (TBST) was used to wash the PVDF membrane. Afterwards, the PVDF membrane was probed by rabbit anti-mouse primary antibodies for 12 h at 4˚C. Rabbit anti-mouse primary antibodies were: p-STING (1:500, AF7416, Fushen Biotechnology, Shanghai, China), p-TBK1 (1:500, NY-1725R-Phospho, Anyan Biotechnology, Nanjing, China), TBK1 (1:1000, ab227182, Abcam, Shanghai, China), p-IRF3 (1:500, ab192796, Abcam, Shanghai, China), IRF3 (1:1000, ab25950, Abcam, Shanghai, China), p-STAT1 (1:500, ab30645, Abcam, Shanghai, China), STAT1 (1:1000, ab47425, Abcam, Shanghai, China) and Actin (1:1000, ab8227, Abcam, Shanghai, China). TBST was used to wash the PVDF membrane again. Horseradish peroxidase-conjugated goat anti-rabbit secondary antibody (1:2000, ab6271, Abcam, Shanghai, China) was added to incubate the PVDF membrane for 2 h at room temperature. Enhanced chemiluminescent (ECL) reagent (Beyotime, Shanghai, China) was applied for protein blots visualization. The density of protein bands were quantified by Image J software (National Institutes of Health, Bethesda, MD, USA). Actin was served as control to normalize other proteins expression.

Statistical analysis

SPSS Software 19.0 was applied for statistical analysis. Data were displayed as mean ± standard deviation. Paired Student's t-test and analysis of variance (followed by Tukey's post hoc test) were utilized respectively for the comparison between two groups and in multiple groups. $P < 0.05$ meant a statistically significant difference. All data were obtained from 3 independent repeated experiments.

Results

Low STING and high PD-1 and PD-L1 proteins expression was exhibited in BCa tissues of patients

IHC was applied to detect STING, PD-1 and PD-L1 proteins expression in BCa tissues and paired adjacent normal tissues of patients. Obviously reduced STING positive particles and increased PD-1 and PD-L1 positive particles were observed in BCa tissues than that in paired adjacent normal tissues (Fig. 1A). Pearson's correlation analysis indicated that, STING mRNA level was negatively correlated with PD-1 mRNA level or PD-L1 mRNA level in BCa tissues of patients (Fig. 1B) ($P < 0.0001$).

STING agonist inhibited BCa cells growth in mice and promoted IFNβ expression in xenograft tumor

In vivo data presented that, mice injected with STING agonist (STING agonist group) showed prominently lower xenograft tumor volume than that injected with PBS (Vehicle group) (Fig. 2A) ($P < 0.001$). ELISA displayed that, xenograft tumor of STING agonist group exhibited markedly higher IFNβ expression level than that of Vehicle group (Fig. 2B) ($P < 0.001$). Western blot indicated that, in contrast with Vehicle group, xenograft tumor of STING agonist group showed significantly higher p-STING, p-TBK1/TBK1, p-IRF3/IRF3 and p-STAT1/STAT1 proteins level (Fig. 2C) ($P < 0.001$).

STING agonist synergized with Atezolizumab to exert anti-tumor effect in BCa mice model

Tumorigenesis ability of 4T1 cells in mice was researched. As displayed in Fig. 3A, in comparison with Vehicle group, the xenograft tumor volume of STING agonist group and Atezolizumab group was both obviously decreased ($P < 0.001$). Relative to STING agonist group, the xenograft tumor volume was significantly reduced in STING agonist + Atezolizumab group ($P < 0.001$).

On the 1st, 7th and 14th day after injection of STING agonist and Atezolizumab, peripheral blood of mice was collected from orbit. The level of TNF-α, IFN-β and IL-10 was detected using ELISA. As a result, compared with Vehicle group, mice of STING agonist group and Atezolizumab group showed obviously higher TNF-α level in peripheral blood on the 1st, 7th and 14th day after administration ($P < 0.01$). On the 7th and 14th day after administration, mice of STING agonist + Atezolizumab group showed much higher TNF-α level than that of STING agonist group ($P < 0.01$). For IFN-β level, it was markedly higher in mice of STING agonist group and Atezolizumab group than that of Vehicle group on the 7th and 14th day after administration ($P < 0.01$). At the same time, much higher IFN-β level was found in mice of STING agonist + Atezolizumab group when relative to STING agonist group ($P < 0.01$). Additionally, matched with Vehicle group, mice of STING agonist group and Atezolizumab group had remarkably higher IL-10 level in peripheral blood on the 1st, 7th and 14th day after administration. At the same time, mice of STING agonist + Atezolizumab group showed prominently higher IL-10 level than that of STING agonist group ($P < 0.05$ or $P < 0.01$) (Fig. 3B).

The level of TNF-α, IFN-β and IL-10 in xenograft tumor was detected by ELISA. Obviously, much higher TNF-α, IFN-β and IL-10 level was detected in STING agonist group and Atezolizumab group when compared to Vehicle group ($P < 0.01$). In contrast with STING agonist group, the TNF-α, IFN-β and IL-10 level was significantly elevated in STING agonist + Atezolizumab group ($P < 0.01$) (Fig. 3C). The mRNA expression of TNF-α, IFN-β and IL-10 in xenograft tumor was further explored by qRT-PCR. As a result, data trend similar to Fig. 3C was occurred (Fig. 3D) ($P < 0.01$).

The level of CD8 + cytotoxic T cells and FOXP3 + Tregs cells in xenograft tumor was investigated by IHC. The photo of IHC indicated that, relative to Vehicle group, more CD8 + positive particles and less FOXP3 +

Tregs positive particles were observed in xenograft tumor of STING agonist group and Atezolizumab group. Matched with STING agonist group, obviously increased CD8 + positive particles and decreased FOXP3 + Tregs positive particles were occurred in xenograft tumor of STING agonist + Atezolizumab group (Fig. 3E).

HE staining exhibited that, the structure of lung, liver, brain-cortex and kidney was similar among Vehicle group, STING agonist group, Atezolizumab group and STING agonist + Atezolizumab group. Cell structure was complete and tissues were arranged in an orderly manner (Fig. 3F). Thus, STING agonist and Atezolizumab were both non-toxic to lung, liver, brain-cortex and kidney.

STING agonist exerted anti-tumor effect in BCa through activating the IFNβ signaling pathway

Phosphorylation level of TBK1, IRF3 and STAT1 in 4T1 cells was investigated by Western blot. The result was displayed in Fig. 4. Matched with Vehicle group, 4T1 cells of STING agonist group presented remarkably higher p-TBK1/TBK1, p-IRF3/IRF3 and p-STAT1/STAT1 level ($P < 0.01$). However, in contrast to STING agonist group, much reduced p-TBK1/TBK1, p-IRF3/IRF3 and p-STAT1/STAT1 level was occurred in 4T1 cells of STING agonist + anti-IFNAR1 group ($P < 0.01$).

Discussion

In this research, STING down-regulation and PD-1 and PD-L1 up-regulation in clinical tissues of BCa patients was revealed by IHC. In vivo study illustrated that STING agonist reduced BCa cells growth in mice. Interestingly, STING agonist synergized with Atezolizumab to enhance anti-tumor efficacy in mice. It should also be noted that, STING agonist and Atezolizumab were both non-toxic to lung, liver, brain-cortex and kidney of BCa mice.

Specifically, STING agonist synergized with Atezolizumab to enhance the expression of TNF-α and IL-10 in peripheral blood and tumor mass of BCa mice. Like other tumors, BCa progression is promoted by inflammation promotion driven by the tumor microenvironment [20]. TNF-α can be expressed by tumor cells themselves, which exerts a dual role in the progression of BCa [20]. On the one hand, it acts as an essential pro-inflammatory cytokines in BCa [21]. On the other hand, excessive TNF-α expression can suppress BCa cells proliferation and tumorigenesis [22]. Thus, in this study, STING agonist might synergize with Atezolizumab to reduce BCa cells growth in mice by overproduction of TNF-α. IL-10 is mainly secreted by activated T-cells, which is an important anti-inflammatory cytokine [23]. It has been reported that STING agonist promoted IL-10 expression to relieve mice with experimental autoimmune encephalomyelitis [24]. This research indicated that STING agonist might synergize with Atezolizumab to exert anti-tumor effect by reducing inflammation via increasing IL-10 expression.

Tumor microenvironment plays an important role in tumor malignant progression, immune escape and treatment resistance [25]. It is well known that the existence of cytotoxic T cells in tumor lesions indicates a well prognosis of patients [26]. CD8 + cytotoxic T cells are considered to be preferred immune cells in

the tumor target treatment. In the process of tumor progression, CD8 + cytotoxic T cells experience dysfunction and exhaustion because of the immunosuppression [27]. Previous study had reported that, in mice tumor model, STING agonist treatment increased CD8 + cytotoxic T cells in tumor mass [28]. In preclinical models, STING agonist induced the local activation of CD8 + cytotoxic T cell in tumor lesions, thereby resulting in tumor regression and durable anti-tumor immunity [29]. Additionally, data in this paper revealed that STING agonist synergized with Atezolizumab to reduce FOXP3 + Tregs cells in BCa tumor mass. FOXP3 + Tregs are important inhibitor of antitumor responses, which can maintain the immunological tolerance to host tissues [30]. High FoxP3 + Tregs infiltration is associated with unfavorable prognosis of tumor patients [31]. In BCa, CD8 + cytotoxic T cells and FoxP3 + Tregs are identified to be potential prognostic factors for patients. High CD8 + cytotoxic T cells infiltration indicated a favorable prognosis, whereas high FoxP3 + Tregs infiltration revealed a poor outcome of BCa patients [32]. This study novel demonstrated that STING agonist synergized with Atezolizumab to increase CD8 + cytotoxic T cells and decrease FoxP3 + Tregs infiltration in BCa tumor mass.

This study discovered that STING agonist synergized with Atezolizumab to increase IFNβ level in peripheral blood and tumor mass of BCa mice. IFNβ was suggested to be used in BCa treatment because of its stimulation of cellular immunity [33]. BCa patients with high IFNβ level were associated with favorable clinical prognosis, such as the repressed cancer stem cells property [34]. In terms of immunotherapy, IFNβ treatment can bridge the immune responses by targeting the tumor microenvironment [35]. Previous study had reported that STING agonist possessed anti-tumor effect in pancreatic cancer by activating the IFN-β pathway [36]. Furthermore, it was noted that STING agonist resulted in the activation of STING, TBK1, IRF3 and STAT1. In tumor microenvironment, the activation of STING, TBK1, IRF3 and STAT1 had been reported to enhance the immune cell infiltration and the sensitivity of tumors to immune checkpoint blockade [37, 38]. However, in vitro study demonstrated that anti-IFNAR1 treatment significantly reversed the promoting effect of STING agonist on the activation of TBK1, IRF3 and STAT1. Thus, it was speculated that STING agonist might synergize with Atezolizumab to enhance immunotherapy effect by activating the IFNβ signaling pathway.

Conclusion

This study investigated the effect of STING agonist on BCa immunotherapy by Atezolizumab. As a result, STING agonist possessed anti-tumor effect in BCa progression. More importantly, STING agonist enhanced Atezolizumab immunotherapy efficacy by activating the IFNβ signaling pathway. Thus, STING agonist could not only be used for BCa treatment, but also could be used in combination with Atezolizumab to enhance the efficacy of immunotherapy.

Declarations

Funding

This work is supported by Scientific Research Program of Anhui Provincial Health and Family Planning Commission (No.2018SEYL019) and Key Natural Science Project of Education Department of Anhui Province (No.KJ2019A1095).

Authors' contributions

Mingming Yin, Jinlong Hu, Wenyong Wu, and Zhiqi Hu designed the study. All author performed the experiments. Jinlong Hu, Wenyong Wu, and Zhiqi Hu analyzed the data. Mingming Yin and Wenyong Wu wrote the manuscript. All authors read and approved the final manuscript.

Data availability

The datasets generated during and/or analyzed during the current study are available from the corresponding author on reasonable request.

Ethical approval

This research has been approved by the ethics committee of Anhiu No.2 Provincial People's Hospital and complied with the Declaration of Helsinki. All patients have signed written informed consent and voluntarily joined the study.

Conflict of interest

No potential conflict of interest was reported by the authors.

References

1. Zhu Q, et al. circSLC8A1 sponges miR-671 to regulate breast cancer tumorigenesis via PTEN/PI3k/Akt pathway. Genomics. 2021;113(1 Pt 1):398–410.
2. Wm Nor W, Chung I, Said N. MicroRNA-548m Suppresses Cell Migration and Invasion by Targeting Aryl Hydrocarbon Receptor in Breast Cancer Cells. Oncol Res. 2021;28(6):615–29.
3. Yuan X, et al. Breast cancer exosomes contribute to pre-metastatic niche formation and promote bone metastasis of tumor cells. Theranostics. 2021;11(3):1429–45.
4. Emens LA. Breast Cancer Immunotherapy: Facts and Hopes. Clin Cancer Res. 2018;24(3):511–20.
5. Tsoukalas N, et al. PD-1 and PD-L1 as immunotherapy targets and biomarkers in non-small cell lung cancer. J buon. 2019;24(3):883–8.
6. Dermani FK, et al., PD-1/PD-L1 immune checkpoint: Potential target for cancer therapy. 2019. 234(2): p. 1313–1325.
7. Jiang Y, et al., PD-1 and PD-L1 in cancer immunotherapy: clinical implications and future considerations. 2019. 15(5): p. 1111–1122.
8. Li C, et al. Peptide Blocking of PD-1/PD-L1 Interaction for Cancer Immunotherapy. Cancer Immunol Res. 2018;6(2):178–88.

9. Nowicki TS, Hu-Lieskovan S, Ribas A. Mechanisms of Resistance to PD-1 and PD-L1 Blockade. Cancer J. 2018;24(1):47–53.
10. Reddy SM, Carroll E, Nanda R. Atezolizumab for the treatment of breast cancer. 2020. 20(3): p. 151–158.
11. Herbst RS, et al. Atezolizumab for First-Line Treatment of PD-L1-Selected Patients with NSCLC. N Engl J Med. 2020;383(14):1328–39.
12. Noguchi E, Shien T, Iwata H. Current status of PD-1/PD-L1 blockade immunotherapy in breast cancer. Jpn J Clin Oncol. 2021;51(3):321–32.
13. Heimes AS, Schmidt M. Atezolizumab for the treatment of triple-negative breast cancer. Expert Opin Investig Drugs. 2019;28(1):1–5.
14. Shae D, Becker KW. Endosomolytic polymersomes increase the activity of cyclic dinucleotide STING agonists to enhance cancer immunotherapy. 2019. 14(3): p. 269–278.
15. Corrales L, et al. The host STING pathway at the interface of cancer and immunity. Journal of Clinical Investigation. 2016;126(7):2404.
16. Chen YP, et al., STING Activator c-di-GMP-Loaded Mesoporous Silica Nanoparticles Enhance Immunotherapy Against Breast Cancer. 2020. 12(51): p. 56741–56752.
17. Yang H, et al. STING activation reprograms tumor vasculatures and synergizes with VEGFR2 blockade. J Clin Invest. 2019;129(10):4350–64.
18. Abd Razak N, Yeap SK, Alitheen NB. Eupatorin Suppressed Tumor Progression and Enhanced Immunity in a 4T1 Murine Breast Cancer Model. 2020. 19: p. 1534735420935625.
19. Roda E, et al., Novel Medicinal Mushroom Blend as a Promising Supplement in Integrative Oncology: A Multi-Tiered Study using 4T1 Triple-Negative Mouse Breast Cancer Model. Int J Mol Sci, 2020. 21(10).
20. Cruceriu D, Baldasici O, Balacescu O. The dual role of tumor necrosis factor-alpha (TNF-α) in breast cancer: molecular insights and therapeutic approaches. 2020. 43(1): p. 1–18.
21. Ma Y, et al. IL-6, IL-8 and TNF-α levels correlate with disease stage in breast cancer patients. Adv Clin Exp Med. 2017;26(3):421–6.
22. Wang K, et al. Tumor Necrosis Factor (TNF)-α-Induced Protein 8-like-2 (TIPE2) Inhibits Proliferation and Tumorigenesis in Breast Cancer Cells. Oncol Res. 2017;25(1):55–63.
23. Fujio K, Yamamoto K, Okamura T. Overview of LAG-3-Expressing, IL-10-Producing Regulatory T Cells. Curr Top Microbiol Immunol. 2017;410:29–45.
24. Johnson BM, et al., STING Agonist Mitigates Experimental Autoimmune Encephalomyelitis by Stimulating Type I IFN-Dependent and -Independent Immune-Regulatory Pathways. 2021. 206(9): p. 2015–2028.
25. Liu M, et al. Understanding the epigenetic regulation of tumours and their microenvironments: opportunities and problems for epigenetic therapy. J Pathol. 2017;241(1):10–24.

26. van der Leun AM, Thommen DS. CD8(+) T cell states in human cancer: insights from single-cell analysis. 2020. 20(4): p. 218–232.
27. Farhood B, Najafi M, Mortezaee K. CD8(+) cytotoxic T lymphocytes in cancer immunotherapy: A review. 2019. 234(6): p. 8509–8521.
28. Ghaffari A, et al. STING agonist therapy in combination with PD-1 immune checkpoint blockade enhances response to carboplatin chemotherapy in high-grade serous ovarian cancer. Br J Cancer. 2018;119(4):440–9.
29. Sivick KE, et al. Magnitude of Therapeutic STING Activation Determines CD8(+) T Cell-Mediated Anti-tumor Immunity. Cell Rep. 2018;25(11):3074–85.e5.
30. Sakaguchi S, et al. Regulatory T cells and immune tolerance. Cell. 2008;133(5):775–87.
31. Shang B, et al. Prognostic value of tumor-infiltrating FoxP3 + regulatory T cells in cancers: a systematic review and meta-analysis. Sci Rep. 2015;5:15179.
32. Peng GL, et al. CD8(+) cytotoxic and FoxP3(+) regulatory T lymphocytes serve as prognostic factors in breast cancer. Am J Transl Res. 2019;11(8):5039–53.
33. Carpi A, et al. Cytokines in the management of high risk or advanced breast cancer: an update and expectation. Curr Cancer Drug Targets. 2009;9(8):888–903.
34. Doherty MR, et al. The opposing effects of interferon-beta and oncostatin-M as regulators of cancer stem cell plasticity in triple-negative breast cancer. Breast Cancer Res. 2019;21(1):54.
35. Yang X, et al. Targeting the tumor microenvironment with interferon-β bridges innate and adaptive immune responses. Cancer Cell. 2014;25(1):37–48.
36. Ren D, et al. Metformin activates the STING/IRF3/IFN-β pathway by inhibiting AKT phosphorylation in pancreatic cancer. Am J Cancer Res. 2020;10(9):2851–64.
37. Sen T, et al., Targeting DNA Damage Response Promotes Antitumor Immunity through STING-Mediated T-cell Activation in Small Cell Lung Cancer. Cancer Discovery, 2019.
38. Zemek RM, De Jong E, Sensitization to immune checkpoint blockade through activation of a STAT1/NK axis in the tumor microenvironment. 2019. 11(501).

Figures

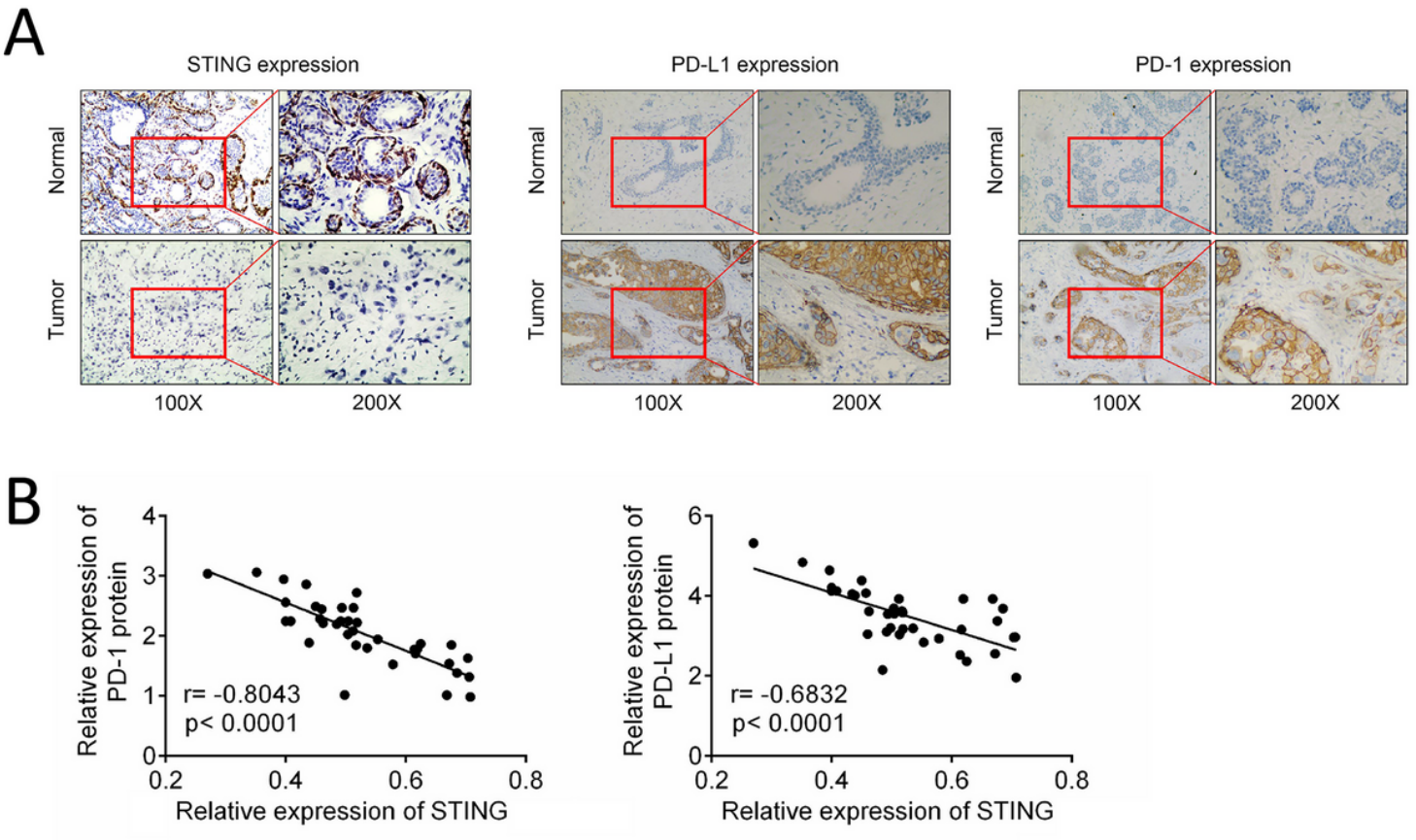

Figure 1

STING was down-regulated and PD-1 and PD-L1 was up-regulated in BCa tissues of patients (A) IHC was performed to detect STING, PD-1 and PD-L1 proteins expression in BCa tissues and paired adjacent normal tissues of patients. (B) Pearson's correlation analysis was conducted to research the correlation between STING protein level and PD-1 protein level or PD-L1 protein level in BCa tissues of patients.

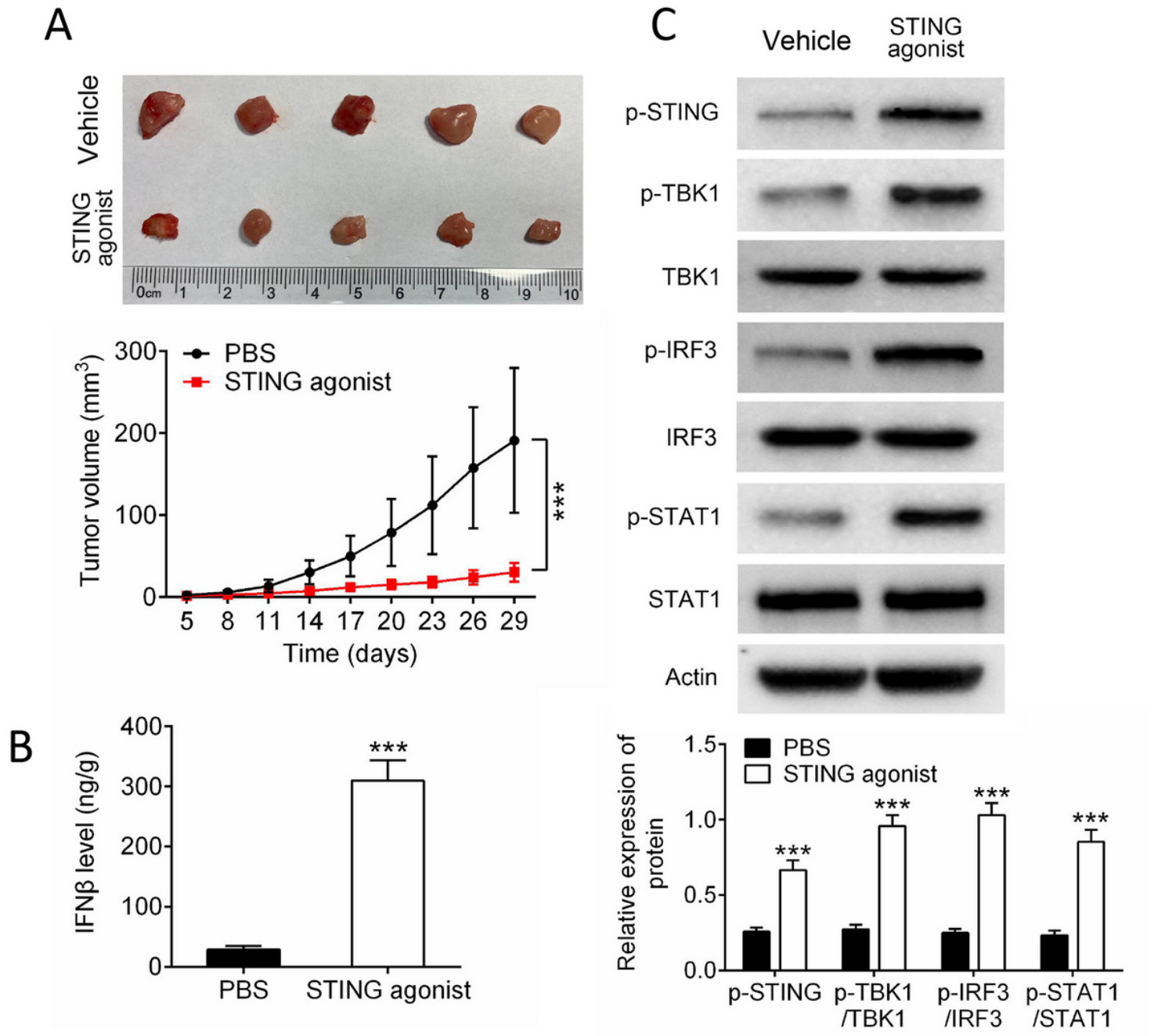

Figure 2

STING agonist inhibited BCa cells growth in mice and promoted IFNβ expression in xenograft tumor (A) Xenograft tumor volume was measured. (B) ELISA was used for IFNβ expression level detection in xenograft tumor. (C) Western blot was applied for proteins expression in xenograft tumor. *** $P < 0.001$.

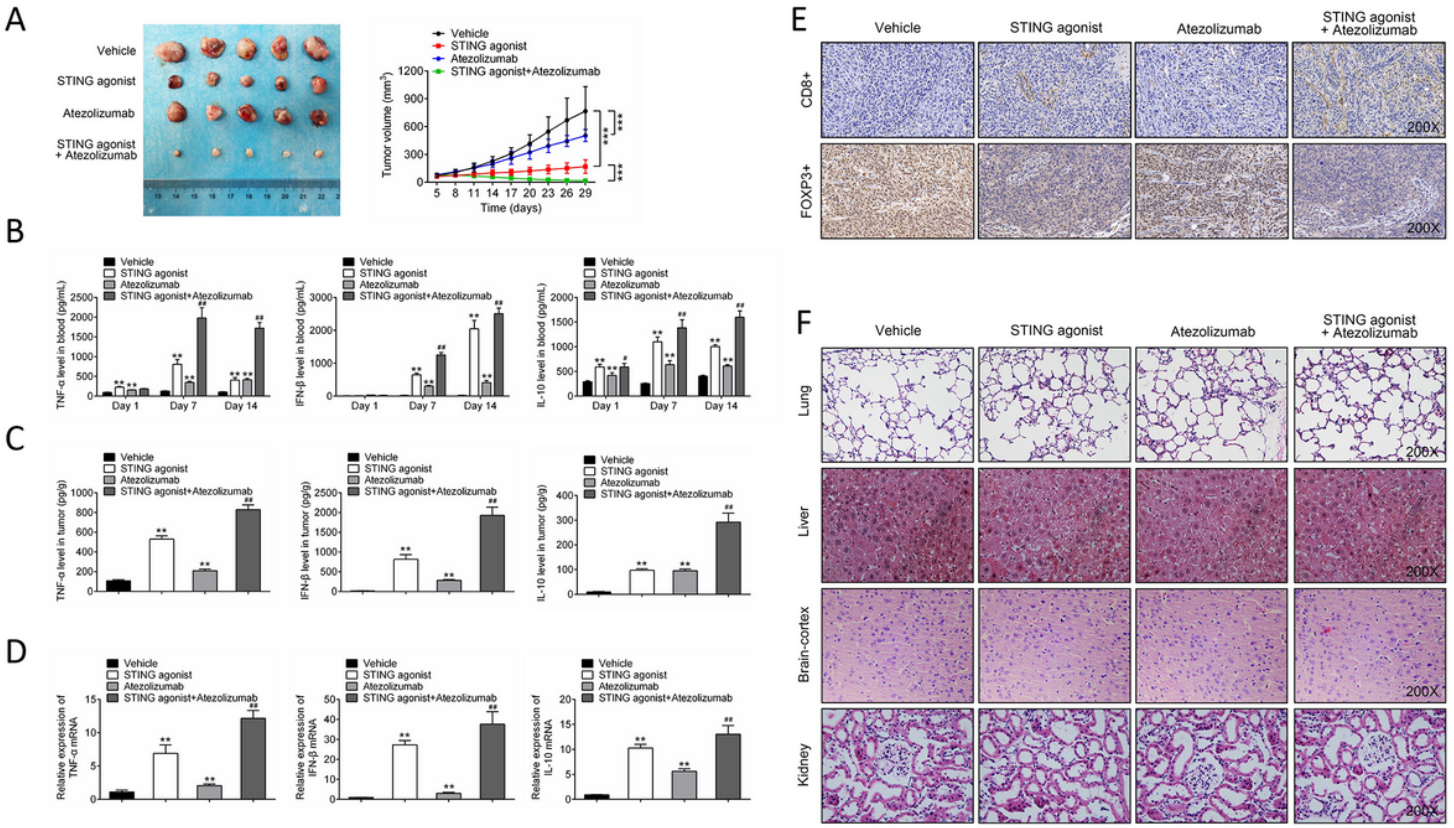

Figure 3

STING agonist synergized with Atezolizumab to exert anti-tumor effect in BCa mice model (A) Xenograft tumor volume was measured. *** P < 0.001. (B) ELISA was performed to detect TNF-α, IFN-β and IL-10 level in mice peripheral blood on the 1st, 7th and 14th day after administration of STING agonist and Atezolizumab. (C) TNF-α, IFN-β and IL-10 level in xenograft tumor was researched by ELISA. (D) TNF-α, IFN-β and IL-10 mRNA expression in xenograft tumor was explored by qRT-PCR. (E) CD8+ cytotoxic T cells and FOXP3+ Tregs cells in xenograft tumor was investigated by IHC. (F) The toxic of STING agonist and Atezolizumab to lung, liver, brain-cortex and kidney of mice was detected by HE staining. ** P < 0.01 vs. Vehicle group. # P < 0.05 and ## P < 0.01 vs. STING agonist group.

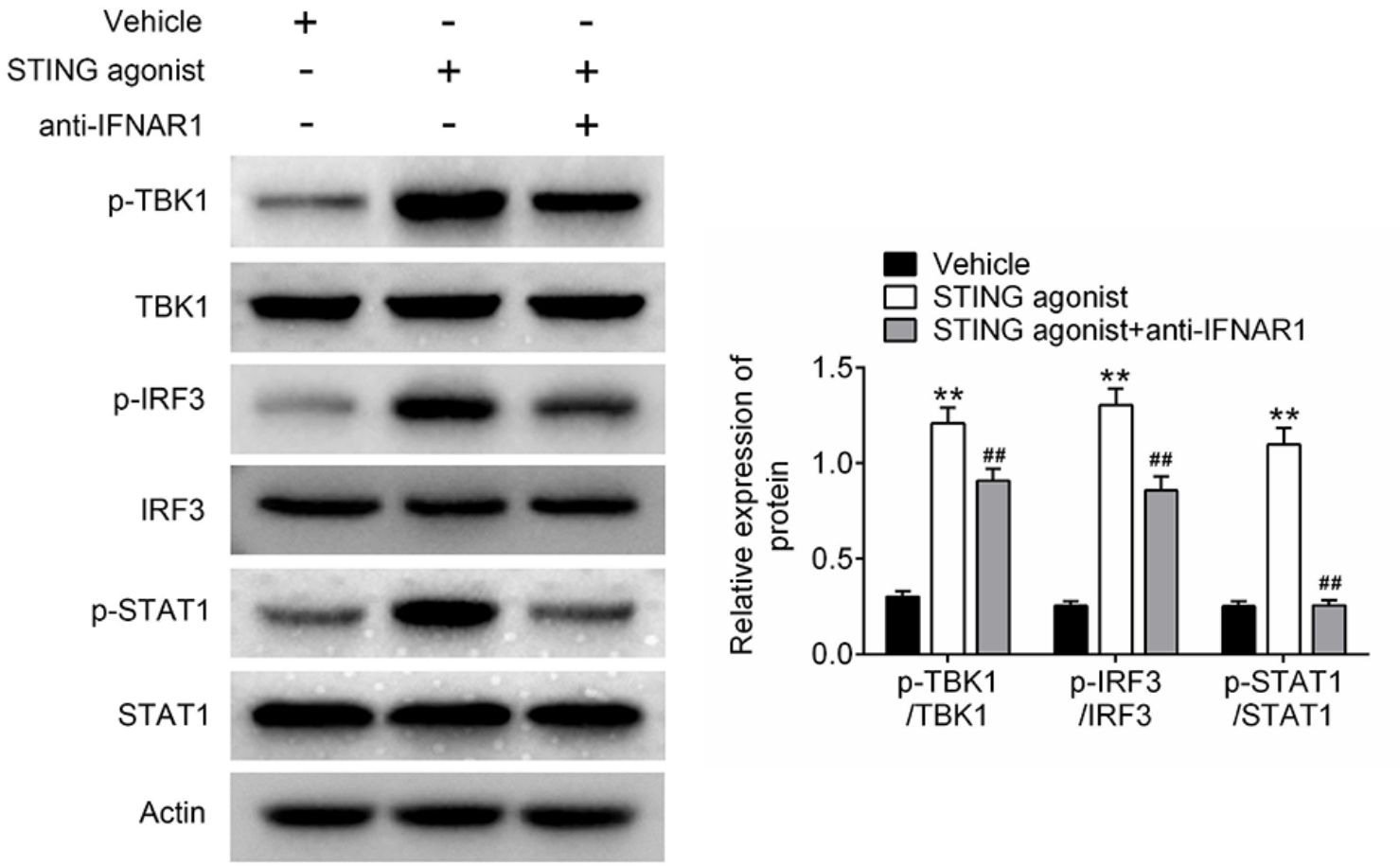

Figure 4

STING agonist exerted anti-tumor effect in BCa through activating the IFNβ signaling pathway ** P < 0.01 vs. Vehicle group. ## P < 0.01 vs. STING agonist group.